ECRONICON OPEN ACCESS

EC OPHTHALMOLOGY
Research Article

Light-Sheet Microscopy of the Optic Nerve Reveals Axonal Degeneration and Microglial Activation in NMDA-Induced Retinal Injury

Yonju Ha[1]*, Lorenzo F Ochoa[2], Olivia Solomon[2,3], Shuizhen Shi[1], Paula P Villarreal[2], Shengguo Li[1], Seth Buscho[1], Gracie Vargas[2]*, Wenbo Zhang[1,2]*

[1]*Department of Ophthalmology and Visual Sciences, University of Texas Medical Branch, Galveston, Texas, USA*

[2]*Department of Neuroscience, Cell Biology and Anatomy, University of Texas Medical Branch, Galveston, Texas, USA*

[3]*Human Pathophysiology and Translational Medicine Graduate Program, University of Texas Medical Branch, Galveston, Texas, USA*

***Corresponding Author:** Wenbo Zhang, Department of Ophthalmology and Visual Sciences, University of Texas Medical Branch, Galveston, Texas, USA, Gracie Vargas, Department of Neuroscience, Cell Biology and Anatomy, University of Texas Medical Branch, Galveston, Texas, USA and Yonju Ha Department of Ophthalmology and Visual Sciences, University of Texas Medical Branch, Galveston, Texas, USA.

Received: October 15, 2021; **Published:** October 28, 2021

Abstract

Purpose: Optic nerve degeneration is a feature of neurodegenerative eye diseases and causes irreversible vision loss. Therefore, understanding the degeneration patterns of the optic nerve is critical to identify potential therapeutic targets for optic neuropathy. However, the traditional method of analyzing optic nerve degeneration by histology has the limitation of losing information about spatiotemporal tissue changes. Light sheet fluorescence microscopy (LSFM) is a fluorescence microscopy technique that allows capturing 3D images rapidly with high spatial optical resolution. In this study, we evaluated the application of LSFM on the optic nerve in a mouse model of N -methyl-D-aspartate (NMDA)-induced retinal injury.

Methods: NMDA or vehicle was injected to the vitreous of Thy1-CFP mice that express cyan fluorescent protein (CFP) in retinal ganglion cells (RGCs) and their axons. At 7 days after the injection, the retina and optic nerve were collected and immunostained with anti-Iba1 antibody. Retinal flatmounts were observed using confocal microscopy. The immunostained optic nerve was optically cleared with 2,2′-Thiodiethanol and mounted for LSFM imaging.

Results: We found significant loss of CFP-expressing RGCs and axon degeneration in retinal flatmounts at 7 days after NMDA injection. These data verified that NMDA induces the loss of RGCs and their axons, NMDA excitotoxicity induced microglial activation and leukostasis, including increased microglia number, the transformation of microglial morphology to amoeboid or rounded shape, and the increase of attached leukocytes to the vessel wall. Using LSFM, we observed that CFP-expressing nerve fiber was well organized and arranged in parallel in vehicle-treated optic nerve. In contrast, in NMDA-treated eyes, optic nerve showed axonal swelling and fragmentation, and loss of axonal density from the proximal to the distal regions. Furthermore, LSFM enabled the observation of microglial phenotypic transformation in the entire optic nerve. In NMDA-treated eyes, microglia displayed larger soma and shorter process with higher Iba1 expression within the entire optic nerve than those in the optic nerve of vehicle-treated eyes.

Conclusion: In summary, we demonstrated the applicability of LSFM to acquire 3D images of the optic nerve and revealed the complex spatial relationships between the axons and microglia within the entire optic nerve by single acquisition. We successfully obtained high-resolution 3D images of NMDA-induced optic neuropathy, including the clues for optic nerve degeneration such as axon swelling, axonal fragmentation, and microglial activation. Our study suggests that LSFM could be a useful technique to investigate the pathology of the optic nerve in neurodegenerative diseases.

Keywords: *Mouse; Retina; Retinal Ganglion Cells; Microglia; Optic Nerve; NMDA; Light Sheet Fluorescence Microscopy*

Introduction

The optic nerve has a critical role in connecting the eye and brain and transmitting the visual signal from the eye to the brain. Optic nerve degeneration is irreversible and is one of the characteristics of neurodegenerative diseases such as glaucoma, diabetes, Alzheimer's disease, Parkinson's disease, Huntington's disease, etc [1-5]. Understanding the pathophysiological changes of optic nerve degeneration is critical to find the potential therapeutic targets for neurodegeneration. The traditional method to analyze optic nerve degeneration relies on confocal imaging which depends on tissue sectioning as depth of imaging is limited to tens of microns. This prohibits true volumetric 3D analysis of the complex tissue structure beyond a few cell layers. Moreover, tissue distortions, axonal fragmentation and loss of 3D spatial relationships among axons, vessels and glia cells may occur during the preparation of thin and flattened optic nerve tissue sections.

In order to analyze tissue with preserved spatial information, techniques allowing for whole-tissue 3D imaging are required. Light sheet fluorescence microscopy (LSFM) with whole-mount optical clearing offers a solution. LSFM is a microscopy technique that enables the rapid capture of 3D images with a high spatial optical resolution but minimal photobleaching and phototoxicity [6-8]. Moreover, unlike confocal microscopy, which relies on point scanning imaging to acquire images, LSFM can rapidly capture 3D images across optical cleared tissue with multiple fluorescent channels due to illumination of planes of light to induce fluorescence in the full plane at once [9,10]. Optical clearing reduces the light scattering of normally turbid tissues to enable deep penetrance of the illumination [11]. Therefore, a technical improvement allowing the study of the optic nerve at high resolution in its entirety can be achieved through the combination of optical clearing and LSMF.

N -methyl-D-aspartate (NMDA)-mediated excitotoxicity plays a role in neurodegenerative diseases [12-14]. In the retina, activation of the NMDA pathway results in retinal ganglion cell (RGC) death and optic neuropathy [15,16]. Intravitreal injection of NMDA is a reliable model to study the excitotoxicity in the retina [15,17-19]. In this study, we combined optical clearing and LSMF to evaluate the pathological changes along the whole optic nerve of intravitreal NMDA-treated mice.

Materials and Methods

Animals

All experimental procedures and use of animals were performed in accordance with the Association of Research for Vision and Ophthalmology Statement for the Use of Animals in Ophthalmic and Vision Research, and animal protocols were approved by the Institutional Animal Care and Use Committee at the University of Texas Medical Branch. B6. Cg-Tg(Thy1-CFP)23Jrs/J (Thy1-CFP mice, Stock number: 003710) were obtained from Jackson Laboratory (Bar Harbor, ME). Mice were maintained on a 12:12 light/dark cycle with food and water available *ad libitum*.

NMDA injection

Mice were anesthetized by intraperitoneal injection with a combination of ketamine (100 mg/kg) and xylazine (10 mg/kg). Eyes were topically dilated with tropicamide and phenylephrine, then 0.5% proparacaine hydrochloride was applied for topical anesthesia. NMDA (160 μM in water, 0.5 μl/eye, Sigma-Aldrich, St. Louis, MO) or vehicle control (water, 0.5 μl/eye) was delivered by intravitreal injection. Then, neomycin ophthalmic ointment was used to prevent eye infection. At 7 days after intravitreal injections, eyes and optic nerves were collected for further analysis.

Leukostasis assay

Leukostasis assay was performed as described previously [20,21]. At 7 days after NMDA intravitreal injection, mice were anesthetized by intraperitoneal injection of a mixture of ketamine (100 mg/kg) and xylazine (10 mg/kg), and the chest cavity was opened. The perfu-

sion cannula was inserted into the left ventricle, and the right atrium was cut for drainage. After phosphate-buffered saline (PBS) was perfused to remove the blood and nonadherent leukocytes, rhodamine-labeled concanavalin A (ConA) lectin (40 μg/mL in PBS, pH 7.4; Vector Laboratories, Burlingame, CA) was perfused to label adherent leukocytes and vessels. Next, PBS was perfused to remove residual unbound Con A. Finally, eyes and optic nerves were collected. The total number of the adherent leukocytes per retina was counted under fluorescent microscopy.

Retinal whole mount staining

After leukostasis assay, eyes were collected and fixed with 4% PFA at 4°C overnight. The next day, retinas were dissected and washed with PBS, and retinas were blocked and permeabilized with PBS containing 5% normal goat serum and 0.3% Triton-X-100 for 3 hours. After blocking, retinas were stained with rabbit anti-Iba1 antibody (1:400, 019-19741, FUJIFILM Wako Chemicals, Richmond, VA) at 4°C overnight. Retinas were washed and incubated with Alexa Fluor 647-conjugated goat anti-rabbit secondary antibody (1:400, Thermo Fisher Scientific, Waltham, MA) at 4°C for 4 hours. At last, retinas were mounted, and images were captured by confocal microscopy (LSM 800, Carl Zeiss Inc, Thornwood, NY).

Optic nerve whole mount staining

After leukostasis assay, optic nerves were collected and fixed with 4% PFA for 5 hours at 4°C and washed with PBS containing 1% Triton (PTX). After blocking with 10% normal goat serum in PTX at 4°C overnight, optic nerves were incubated with an anti-Iba1 antibody (1:100) for 72 hours at 4°C. Subsequently, optic nerves were washed with PTX for 6 hours at room temperature, and PTX was changed every hour. Then, optic nerves were incubated with Alexa Fluor 647-conjugated secondary antibody (1:200) at 4°C for 48 hours and washed with PTX for 6 hours at room temperature with changing the PTX every hour, and then washed with PTX overnight at 4°C.

Optic nerve optical clearing

Optic nerves were cleared by incubating in increasing concentrations (from 10% to 70%) of 2,2′-Thiodiethanol (TDE, 88561-2.5L, Sigma-Aldrich) at 10% intervals and 0.5% dimethyl sulfoxide (DMSO, 472301-500ML, Sigma-Aldrich). Optic nerves were incubated for 1 hour in each concentration, with 70% mixture being refreshed for microscopy mounting.

Light sheet fluorescent microscopy (LSMF) imaging

Samples were embedded in 1% agarose (16520100, Thermo Fisher Scientific) and held inside a glass capillary with Teflon plunger (Sutter Instruments). Imaging was performed with a Zeiss Lightsheet Z.1 (Carl Zeiss AG, Jena, Germany) with 5X and 20X objectives with lasers centered at 445 nm, 561 nm, and 638 nm. Acquisitions used dual sided light sheet illumination with images captured using a dual detector setup (PCO.Edge sCMOS, Wilmington, DE). ZEN Black software was used for acquisition and ZEN Lite with arivis Vision4D) for visualization and 3D reconstructions. Image processing and final image reconstructions were made using FIJI/ImageJ software (v1.53M, NIH Image) and Imaris 3D analysis software (v9.72, Bitplane, Belfast, United Kingdom).

Statistics

Data were presented as mean ± standard error of mean (SEM) and analyzed by student's t-test. Statistical analysis was conducted using GraphPad Prism program (GraphPad Software Inc., La Jolla, CA). A p value < 0.05 was considered statistically significant.

Results

NMDA excitotoxicity induced degeneration of RGCs and their axons accompanied by microglial activation and vascular inflammation in the retina.

Thy1-CFP mice express Cyan Fluorescent Protein (CFP) under the Thy1 promoter, therefore RGC and its axon are labeled with CFP across the retina and optic nerve, allowing the evaluation of RGC and its axonal loss by fluorescence microscopy in acute or chronic eye injuries [22-28]. We intravitreally injected NMDA to Thy1-CFP mice to characterize NMDA excitotoxicity in the retina. Since the retina is transparent and can be flat mounted, we directly observed retinal changes using confocal microscopy with our well-established protocols [20,21,29,30]. We found that there was 53% loss of CFP-expressing RGCs in Thy1-CFP mice at 7 days after NMDA injection (Figure 1A). Moreover, thinner axonal fiber and a significant decrease of axonal bundle number were observed in the central retina of NMDA-treated mice (Figure 1B).

Microglial morphology represents different activation states. When activated, ramified quiescent microglia with thin process changes to rounded morphology or amoeboid morphology with larger soma and shorter processes. We examined the changes of microglia by labeling them with anti-Iba1 antibody [30]. We found that microglial cell number was increased and their morphology was changed from ramified structure to amoeboid or rounded shape with more hypertrophic processes in NMDA-treated retina, indicating that NMDA excitotoxicity also increased microglial recruitment and activation (Figure 1C). Because leukostasis is a major complement of an inflammatory response [20,21,29], we labeled retinal vascular structure and leukocytes adherent to vessel walls with rhodamine-conjugated concanavalin A lectin (Con A). We found there were no noted changes in retinal vasculature. However, the number of adherent leukocytes was significantly increased in the retina after NMDA injection. Taken together, these data indicate that NMDA treatment not only induces RGC loss and axonal degeneration but also causes significant inflammation in the retina.

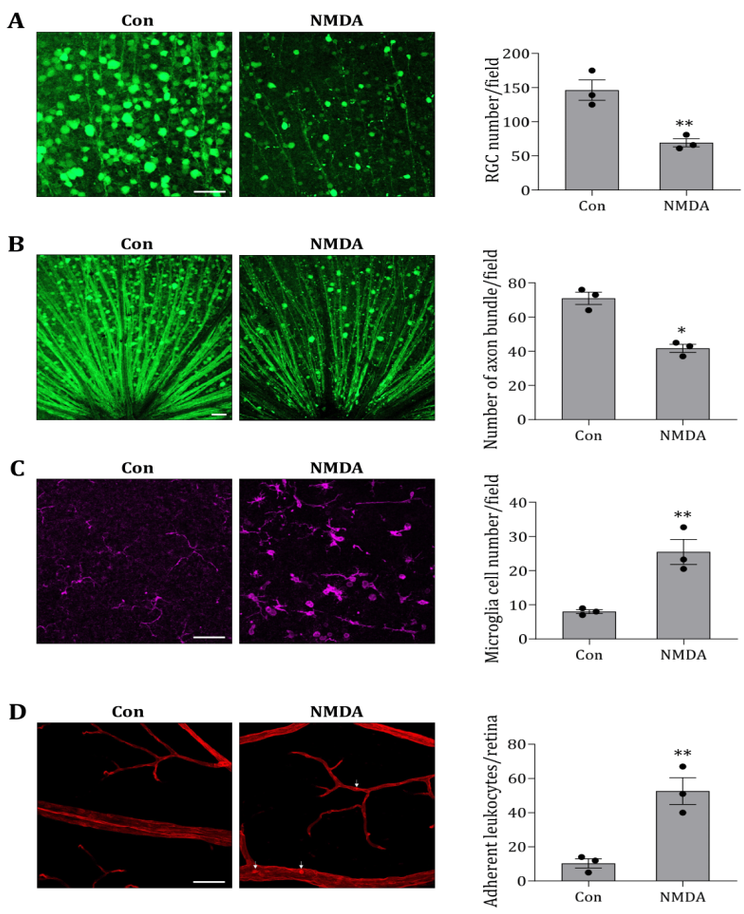

Figure 1: *NMDA induces RGC and its axon loss, microglial activation, and increased leukostasis. NMDA was intravitreally introduced to the eye of Thy1-CFP mice. At 7 days after NMDA injection, retinas were immunostained with anti-Iba1 antibody after leukostasis assay. Representative images of RGC loss in the peripheral retina (A), axonal loss in the central retina (B), microglial activation in the peripheral retina (C), leukostasis in the central retina (D). Green: CFP expressing RGC and axon. Purple: Microglia. Red: ConA labeled vasculature and adherent leukocyte. Arrow indicates adherent leukocytes to the vessel. Bar graphs represent the quantified data. Scale bar = 50 μm. n = 3 per group. *p < 0.05, **p < 0.01.*

LSFM enables 3D imaging of the patterns of NMDA induced axon degeneration and microglia activation in the optic nerve.

Since LSFM is a fluorescence microscopy technique that is able to acquire deep tissue images with 3D information of the entire optically cleared organ, we utilized it to analyze axon degeneration and microglial activation in the optic nerve at 3 different regions (proximal (close to eye globe), middle, and distal (close to chiasma)) at 7 days after NMDA injection. In vehicle-treated eyes, we observed that CFP-expressing nerve fibers were well organized and arranged in parallel in the whole optic nerve (Figure 2A). In contrast, in NMDA-treated eyes, the optic nerve showed axonal swelling and fragmentation, and marked loss of axons from the proximal to the distal regions (Figure 2B). Furthermore, using LSFM, we were able to observe an increase in microglial cell number and distinguish microglial phenotypic changes in NMDA-injected optic nerve, such as larger soma and shorter process with higher Iba1 expression from the proximal to distal regions of the optic nerve than those in the optic nerve of vehicle-treated eyes (Figure 2B). We did not observe vascular change and leukocyte attachment to the vessel in the optic nerve. These results suggest that LSFM will help explore optic nerve pathological changes in diseases by providing detailed 3D information of optic nerve, including axon's morphology and density, microglial number and morphology, and vasculature.

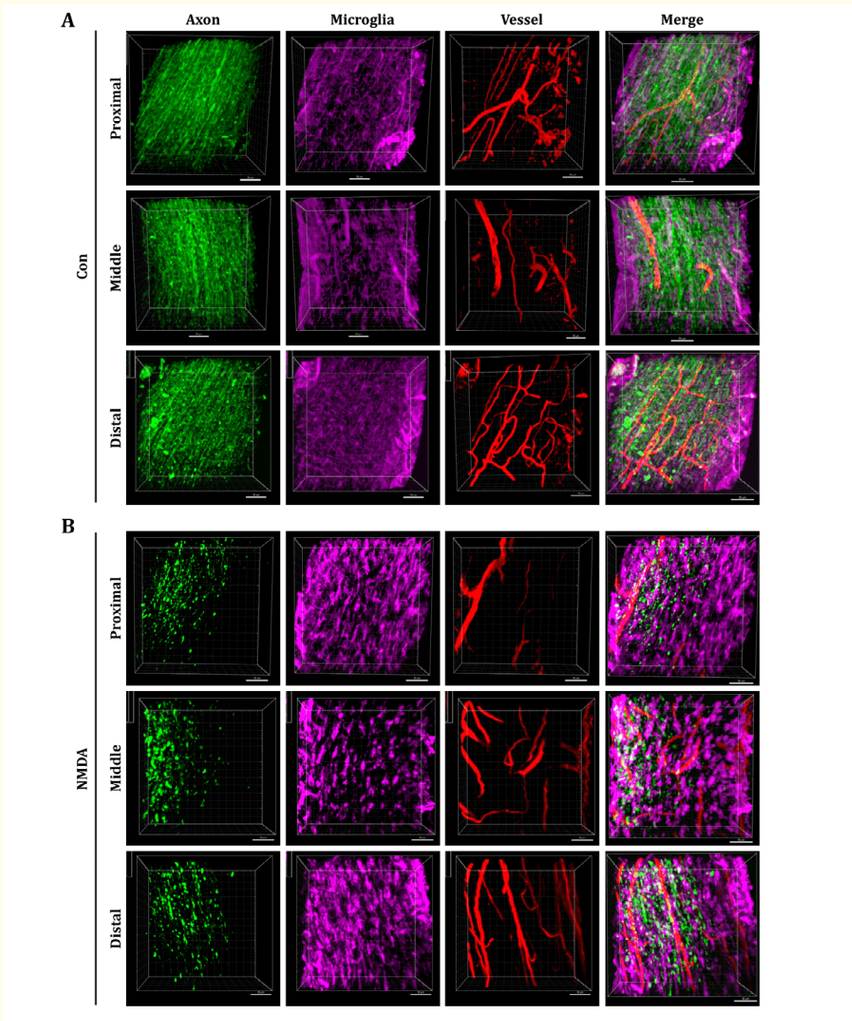

Figure 2: *3D imaging of the patterns of NMDA-induced axon degeneration and microglial activation in the optic nerve. At 7 days after NMDA intravitreal injection to the eye of Thy1-CFP mice, optic nerves were immunostained with anti-Iba1 antibody after leukostasis assay. (A) Representative images of LSFM images in proximal, middle, and distal regions of vehicle-injected optic nerve. (B) Representative images of LSFM images in proximal, middle, and distal regions of NMDA-injected optic nerve. Green: CFP expressing axon. Purple: Microglia. Red: ConA labeled vasculature. Scale bar = 50 µm. n = 3 per group.*

Discussion and Conclusion

RGC loss and optic nerve degeneration cause irreversible vision loss in eye diseases. NMDA-mediated excitotoxicity is a common pathway in neurodegenerative diseases [12-14,31]. Consistent with previous reports, we confirmed that NMDA treatment induced RGC and

its axon loss in the retina. In addition, we found NMDA induced recruitment and activation of microglia and vascular inflammation in the retina. Using optic clearing and LSFM, we succeeded in acquiring high-resolution 3D images at three regions in the whole optic nerve and identified striking changes including axonal swelling, fragmentation and degeneration, and microglial activation. The concurrent changes in the retina and optic nerve suggest a close connection and communication between them during retinal neuronal injury. Future studies are needed to understand its underlying mechanisms.

A suitable optical clearing technique can reduce light scattering, absorption and allow for whole tissue imaging. Recently several studies have reported optical clearing protocols such as ScaleS, SeeDB, CLARITY, 3DISCO, Clear T, and CUBIC, which are able to acquire deep tissue images of an entire organ without losing spatiotemporal information by tissue sectioning [32-37]. Although these methods have been used for other organs, their compatibility with the optic nerve has not been evaluated yet. Among tissue clearing methods, 2,2'-thiodiethanol (TDE) is inexpensive and compatible with immunostaining by not quenching the fluorescence of fluorophores [38]. Moreover, the incremental use of TDE concentrations allows for a gradual penetration of TDE to equalize the tissue's refractive index while avoiding tissue deformation that is seen in some other optical clearing methods [39]. These steps allow for completion of tissue clearing in less than 2 days compared to other methods taking up to 7 days. In this study, we tested the modified TDE exchange method for optic nerve tissue clearing and found that this protocol successfully enabled the imaging of the entire optic nerve using LSFM without tissue distortions and loss of fluorescent information.

LSFM is a powerful tool to capture deep tissue images of the whole organ with preserved spatial tissue information. In addition, LSFM could capture high resolution 3D images with multiple fluorescent channels across the entire tissue with low photobleaching and phototoxicity, overcoming the common limitations of confocal microscopy [6-10]. Due to these advantages of LSFM, several studies have reported the benefits of LSFM in organ imaging such as brain, heart, and kidney, etc [40,41]. However, its feasibility for optic nerve imaging remains little explored. Our data suggest that LSFM will help explore therapeutic targets for vision restoration by providing detailed 3D information of the optic nerve.

In summary, LSFM is applicable to acquire 3D images of the optic nerve and revealed the complex spatial relationships between the axons and microglia within the entire optic nerve by single acquisition. High-resolution 3D images of NMDA-induced optic neuropathy were successfully obtained, including the clues for optic nerve degeneration such as axon swelling, axonal fragmentation, and microglial activation. Therefore, LSFM could be a useful technique to investigate the pathology of the optic nerve in neurodegenerative diseases.

Acknowledgments

This work was supported in part by National Institutes of Health grant EY022694 and EY026629, Retina Research Foundation, and UT System Faculty STARs Award (to W.Z.); National Institutes of Health grant NS106597 and CA247595 (to. G.V.); NIEHS T32 Training Grant Support T32ES007254 (to L. F. O.); Jeane B. Kempner Fellowship Program (to O.S.); and JSME/Tobacco Funds (to Y. H.).

Conflict of Interest Statement

There is no financial interest or conflict of interest.

Authors Contribution

Both authors Yonju Ha and Lorenzo F Ochoa contributed equally for this study.

Bibliography

1. Morrison JC., *et al.* "Pathophysiology of human glaucomatous optic nerve damage: insights from rodent models of glaucoma". *Experimental Eye Research* 93.2 (2011): 156-164.
2. Giuliari GP., *et al.* "Diabetic papillopathy: current and new treatment options". *Current Diabetes Reports* 7.3 (2011): 171-175.
3. La Morgia C., *et al.* "Melanopsin retinal ganglion cell loss in Alzheimer disease". *Annals of Neurology* 79.1 (2016): 90-109.
4. Yu JG., *et al.* "Retinal nerve fiber layer thickness changes in Parkinson disease: a meta-analysis". *PLoS One* 9.1 (2014): e85718.
5. Kersten HM., *et al.* "Optical coherence tomography findings in Huntington's disease: a potential biomarker of disease progression". *Journal of Neurolog* 262.11 (2015): 2457-2465.
6. Prahst C., *et al.* "Mouse retinal cell behaviour in space and time using light sheet fluorescence microscopy". *Elife* (2020): 9.
7. Henning Y., *et al.* "Optical clearing and imaging of immunolabeled mouse eyes using light-sheet fluorescence microscopy". *Experimental Eye Research* 180 (2019): 137-145.
8. Singh JN., *et al.* "Quantifying three-dimensional rodent retina vascular development using optical tissue clearing and light-sheet microscopy". *Journal of Biomedical Optics* 22.7 (2017): 76011.
9. Ding Y., *et al.* "Multiscale light-sheet for rapid imaging of cardiopulmonary system". *JCI Insight* 3.16 (2018).
10. Stelzer EH. "Light-sheet fluorescence microscopy for quantitative biology". *Nature Methods* 12.1 (2015): 23-26.
11. Ueda HR., *et al.* "Whole-Brain Profiling of Cells and Circuits in Mammals by Tissue Clearing and Light-Sheet Microscopy". *Neuron* 106.3 (2020): 369-387.
12. Wang R and PH Reddy. "Role of Glutamate and NMDA Receptors in Alzheimer's Disease". *Journal of Alzheimer's Disease* 57.4 (2017): 1041-1048.
13. Harada T., *et al.* "The potential role of glutamate transporters in the pathogenesis of normal tension glaucoma". *Journal of Clinical Investigation* 117.7 (2007): 1763-1770.
14. Parsons M and LA Raymond. "Extrasynaptic NMDA receptor involvement in central nervous system disorders". *Neuron* 82.2 (2014): 279-293.
15. Siliprandi R., *et al.* "N-methyl-D-aspartate-induced neurotoxicity in the adult rat retina". *Visual Neuroscience* 8.6 (1992): 567-573.
16. Joo CK., *et al.* "Necrosis and apoptosis after retinal ischemia: involvement of NMDA-mediated excitotoxicity and p53". *Investigative Ophthalmology and Visual Science* 40.3 (1999): 713-720.
17. Lucas DR and J Newhouse. "The toxic effect of sodium L-glutamate on the inner layers of the retina". *The Archives of Ophthalmology* 58.2 (1957): 193-201.
18. Manabe S and SA Lipton. "Divergent NMDA signals leading to proapoptotic and antiapoptotic pathways in the rat retina". *Investigative Ophthalmology and Visual Science* 44.1 (2003): 385-392.
19. Gao L., *et al.* "Exploration of the glutamate-mediated retinal excitotoxic damage: a rat model of retinal neurodegeneration". *International Journal of Ophthalmology-IJO* 11.11 (2018): 1746-1754.

20. Liu W., *et al.* "Neuroprotective Effects of HSF1 in Retinal Ischemia-Reperfusion Injury". *Investigative Ophthalmology and Visual Science* 60.4 (2019): 965-977.

21. Liu W., *et al.* "Neuronal Epac1 mediates retinal neurodegeneration in mouse models of ocular hypertension". *Journal of Experimental Medicine* 217.4 (2020).

22. Leung CK., *et al.* "In vivo imaging of murine retinal ganglion cells". *Journal of Neuroscience Methods* 168.2 (2008): 475-478.

23. Feng G., *et al.* "Imaging neuronal subsets in transgenic mice expressing multiple spectral variants of GF". *Neuron* 28.1 (2000): 41-51.

24. Raymond ID., *et al.* "Cyan fluorescent protein expression in ganglion and amacrine cells in a thy1-CFP transgenic mouse retina". *Molecular Vision* 14 (2008): 1559-1574.

25. Chauhan BC., *et al.* "Longitudinal in vivo imaging of retinal ganglion cells and retinal thickness changes following optic nerve injury in mice". *PLoS One* 7.6 (2012): e40352.

26. Leung CK., *et al.* "Longitudinal profile of retinal ganglion cell damage after optic nerve crush with blue-light confocal scanning laser ophthalmoscopy". *Investigative Ophthalmology and Visual Science* 49.11 (2008): 4898-4902.

27. Leung CK., *et al.* "Longitudinal profile of retinal ganglion cell damage assessed with blue-light confocal scanning laser ophthalmoscopy after ischaemic reperfusion injury". *British Journal of Ophthalmology* 93.7 (2009): 964-968.

28. Murata H., *et al.* "Imaging mouse retinal ganglion cells and their loss in vivo by a fundus camera in the normal and ischemia-reperfusion model". *Investigative Ophthalmology and Visual Science* 49.12 (2008): 5546-5552.

29. Xia F., *et al.* "Early alterations of neurovascular unit in the retina in mouse models of tauopathy". *Acta Neuropathologica Communications* 9.1 (2021): 51.

30. Li Y., *et al.* "Zika virus induces neuronal and vascular degeneration in developing mouse retina". *Acta Neuropathologica Communications* 9.1 (2021): 97.

31. Christensen I., *et al.* "The Susceptibility of Retinal Ganglion Cells to Glutamatergic Excitotoxicity Is Type-Specific". *Frontiers in Neuroscience* 13 (2019): 219.

32. Hama H., *et al.* "Scale: a chemical approach for fluorescence imaging and reconstruction of transparent mouse brain". *Nature Neuroscience* 14.11 (2011): 1481-1488.

33. Ke MT., *et al.* "SeeDB: a simple and morphology-preserving optical clearing agent for neuronal circuit reconstruction". *Nature Neuroscience* 16.8 (2013): 1154-1161.

34. Tomer R., *et al.* "Advanced CLARITY for rapid and high-resolution imaging of intact tissues". *Nature Protocols* 9.7 (2014): 1682-1697.

35. Erturk A., *et al.* "Three-dimensional imaging of solvent-cleared organs using 3DISCO". *Nature Protocols* 7.11 (2012): 1983-1995.

36. Susaki EA., *et al.* "Whole-brain imaging with single-cell resolution using chemical cocktails and computational analysis". *Cell* 157.3 (2014): 726-739.

37. Kuwajima T., *et al.* "ClearT: a detergent- and solvent-free clearing method for neuronal and non-neuronal tissue". *Development* 140.6 (2013): 1364-1368.

38. Aoyagi Y., *et al.* "A rapid optical clearing protocol using 2,2'-thiodiethanol for microscopic observation of fixed mouse brain". *PLoS One* 10.1 (2015): e0116280.

39. Xu N., *et al.* "Fast free-of-acrylamide clearing tissue (FACT)-an optimized new protocol for rapid, high-resolution imaging of three-dimensional brain tissue". *Scientific Reports* 7.1 (2017): 9895.

40. Shanahan CM., *et al.* "Arterial calcification in chronic kidney disease: key roles for calcium and phosphate". *Circulation Research* 109.6 (2011): 697-711.

41. Dodt HU., *et al.* "Ultramicroscopy: three-dimensional visualization of neuronal networks in the whole mouse brain". *Nature Methods* 4.4 (2007): 331-336.

Volume 12 Issue 11 November 2021